



LUND UNIVERSITY

Circuit analogs for stratified structures

Sjöberg, Daniel

2007

[Link to publication](#)

Citation for published version (APA):

Sjöberg, D. (2007). *Circuit analogs for stratified structures*. (Technical Report LUTEDX/(TEAT-7159)/1-18/(2007); Vol. TEAT-7159). [Publisher information missing].

Total number of authors:

1

General rights

Unless other specific re-use rights are stated the following general rights apply:

Copyright and moral rights for the publications made accessible in the public portal are retained by the authors and/or other copyright owners and it is a condition of accessing publications that users recognise and abide by the legal requirements associated with these rights.

- Users may download and print one copy of any publication from the public portal for the purpose of private study or research.
- You may not further distribute the material or use it for any profit-making activity or commercial gain
- You may freely distribute the URL identifying the publication in the public portal

Read more about Creative commons licenses: <https://creativecommons.org/licenses/>

Take down policy

If you believe that this document breaches copyright please contact us providing details, and we will remove access to the work immediately and investigate your claim.

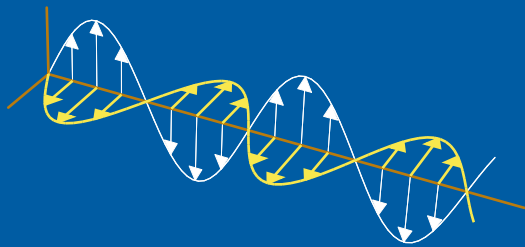
LUND UNIVERSITY

PO Box 117
221 00 Lund
+46 46-222 00 00

Circuit analogs for stratified structures

Daniel Sjöberg

Electromagnetic Theory
Department of Electrical and Information Technology
Lund University
Sweden



Daniel Sjöberg
Daniel.Sjoberg@eit.lth.se

Department of Electrical and Information Technology
Electromagnetic Theory
P.O. Box 118
SE-221 00 Lund
Sweden

Editor: Gerhard Kristensson
© Daniel Sjöberg, Lund, December 20, 2007

Abstract

We present an overview of how circuit models can be used for wave propagation in stratified structures. Homogeneous slabs are modeled as transmission lines, and thin sheets between the slabs are modeled as lumped elements. It is seen that electric material properties contribute as shunt elements, and magnetic material properties contribute as series elements. When the sheets have periodic patterns, they can be represented with resonant circuits. The circuit models should be used as a starting point, to derive a basic, stable design, which can later be optimized using full wave simulations if necessary.

1 Introduction

An absorbing structure can have a quite complicated geometry, which is very time consuming to analyze in full. In the design phase of product development, it is necessary to have fast, yet reasonably accurate, means of evaluating the performance. For absorbers based on a stratified structure, circuit analogs provide such a means.

The circuit analog absorber is more of a design paradigm than a class of absorbers of their own. The idea is to build simple models, which can be used to find an overall basic design that meets demands such as total height and weight of the absorber. Once this basic design is reached, one can go to full wave simulations and more accurate modeling.

The purpose of this paper is to present the underlying theory, *i.e.*, to show why circuit analogs are good models for stratified geometries and how they are connected to the full Maxwell's equations. For more on the design technique, we refer to the books [3, 5, 6] and the paper [7], which deals with the oblique incidence. Also, classical texts on microwave circuits, including matching theory, are of great value when going through the circuit design phase. See for instance [2, 8], and also [1, 4] for analytical expressions for circuit parameters for simple structures.

2 Bulk material as transmission lines

Maxwell's equations for an isotropic material, modelled by a permittivity ϵ and a permeability μ , can be written in terms of the transverse components \mathbf{E}_t and \mathbf{H}_t as (time convention $e^{j\omega t}$)

$$\frac{\partial \mathbf{E}_t}{\partial z} = -\left(j\omega\mu - \frac{1}{j\omega}\nabla_t\epsilon^{-1}\nabla_t\right) \cdot (-\hat{\mathbf{z}} \times \mathbf{H}_t) \quad (2.1)$$

$$\frac{\partial \mathbf{H}_t}{\partial z} = -\left(j\omega\epsilon - \frac{1}{j\omega}\nabla_t\mu^{-1}\nabla_t\right) \cdot (\hat{\mathbf{z}} \times \mathbf{E}_t) \quad (2.2)$$

where $\nabla_t = \hat{\mathbf{x}}\frac{\partial}{\partial x} + \hat{\mathbf{y}}\frac{\partial}{\partial y}$. When considering bulk materials, there is no variation in the transverse plane and the field depends on x and y only through a factor $e^{-j\mathbf{k}_t \cdot (x\hat{\mathbf{x}} + y\hat{\mathbf{y}})}$,

which transforms the equations into (using a dyadic notation)

$$\frac{\partial \mathbf{E}_t}{\partial z} = - \left(j\omega\mu \mathbf{I} + \frac{\mathbf{k}_t \mathbf{k}_t}{j\omega\epsilon} \right) \cdot (-\hat{\mathbf{z}} \times \mathbf{H}_t) = -j\omega\mu \left(\mathbf{I} - \frac{\mathbf{k}_t \mathbf{k}_t}{\omega^2 \epsilon \mu} \right) \cdot (-\hat{\mathbf{z}} \times \mathbf{H}_t) \quad (2.3)$$

$$\frac{\partial \mathbf{H}_t}{\partial z} = - \left(j\omega\epsilon \mathbf{I} + \frac{\mathbf{k}_t \mathbf{k}_t}{j\omega\mu} \right) (\hat{\mathbf{z}} \times \mathbf{E}_t) = -j\omega\epsilon \left(\mathbf{I} - \frac{\mathbf{k}_t \mathbf{k}_t}{\omega^2 \epsilon \mu} \right) \cdot (\hat{\mathbf{z}} \times \mathbf{E}_t) \quad (2.4)$$

There are two sets of solutions to these equations, depending on the direction of the tangential electric and magnetic field relative the vector \mathbf{k}_t :

$$\text{TE: } \mathbf{E}_t \perp \mathbf{k}_t \text{ and } \mathbf{H}_t \parallel \mathbf{k}_t \quad (2.5)$$

$$\text{TM: } \mathbf{E}_t \parallel \mathbf{k}_t \text{ and } \mathbf{H}_t \perp \mathbf{k}_t \quad (2.6)$$

In lossless media $\omega^2 \epsilon \mu$ is the square of the total wave number. This motivates us to define the angle θ by

$$\cos^2 \theta = 1 - \frac{|\mathbf{k}_t|^2}{\omega^2 \epsilon \mu} \quad (2.7)$$

which is a complex angle if the material parameters are complex. In lossless media it is real for propagating waves, and represents the angle of the propagation direction with the z axis.

Identifying the transverse fields as the voltage and current as $\mathbf{E}_t \leftrightarrow V$ and $-\hat{\mathbf{z}} \times \mathbf{H}_t \leftrightarrow I$, respectively, this means we have two sets of equations,

$$\frac{\partial V}{\partial z} = -j\omega\mu \left\{ \begin{array}{c} 1 \\ \cos^2 \theta \end{array} \right\} I \quad (2.8)$$

$$\frac{\partial I}{\partial z} = -j\omega\epsilon \left\{ \begin{array}{c} \cos^2 \theta \\ 1 \end{array} \right\} V \quad (2.9)$$

where the upper alternative corresponds to TE polarization, and the lower alternative corresponds to TM polarization. This resembles the traditional transmission line equations,

$$\frac{\partial V}{\partial z} = -(j\omega L + R)I = -\gamma Z_0 I \quad (2.10)$$

$$\frac{\partial I}{\partial z} = -(j\omega C + G)V = -\gamma Y_0 V \quad (2.11)$$

where L , R , C , and G are the distributed circuit parameters of the transmission line, $\gamma = \sqrt{(j\omega L + R)(j\omega C + G)}$ is the propagation constant of the transmission line, and $Z_0 = 1/Y_0 = \sqrt{(j\omega L + R)/(j\omega C + G)}$ is the characteristic impedance of the transmission line. This means we can identify distributed circuit parameters from the permeability and permittivity according to

$$j\omega L + R = (j\omega\mu' + \omega\mu'') \left\{ \begin{array}{c} 1 \\ \cos^2 \theta \end{array} \right\} \quad (2.12)$$

$$j\omega C + G = (j\omega\epsilon' + \omega\epsilon'') \left\{ \begin{array}{c} \cos^2 \theta \\ 1 \end{array} \right\} \quad (2.13)$$

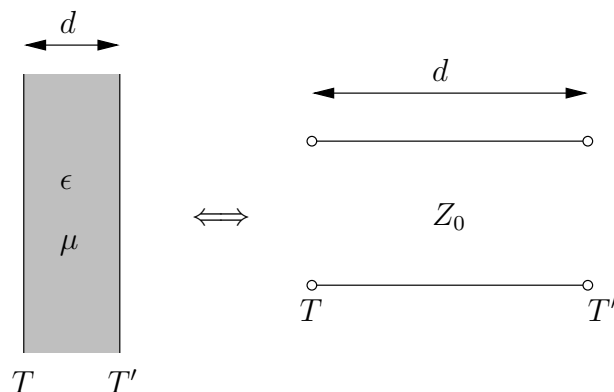


Figure 1: Transmission line model of a bulk slab.

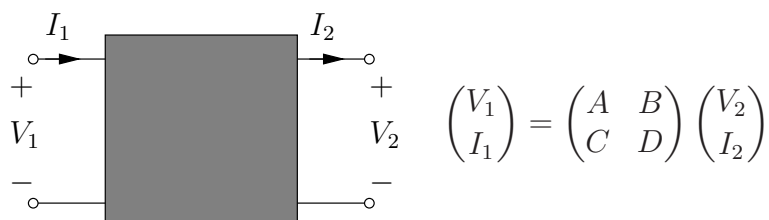


Figure 2: Definition of the voltage-current transmission matrix (ABCD matrix) for a two-port network. Note that the ABCD matrix can be cascaded, *i.e.*, if two networks are connected together, the total ABCD matrix is the product of the individual matrices.

where we used the decompositions $\mu = \mu' - j\mu''$ and $\epsilon = \epsilon' - j\epsilon''$. Note that if the material parameters ϵ and μ depend on frequency, so will the identified circuit parameters. The propagation constant is

$$\gamma = \sqrt{(j\omega L + R)(j\omega C + G)} = \sqrt{(j\omega\mu' + \omega\mu'')(j\omega\epsilon' + \omega\epsilon'') \cos^2 \theta} = jk \cos \theta \quad (2.14)$$

where $k = \omega\sqrt{\epsilon\mu}$ is the intrinsic wave number. The scaling of the wavenumber by $\cos \theta$ means the wavelength on the line is $\lambda_g = \lambda / \cos \theta$, where λ is the intrinsic wavelength. The characteristic impedance is

$$Z_0 = \sqrt{\frac{j\omega L + R}{j\omega C + G}} = \sqrt{\frac{j\omega\mu' + \omega\mu''}{j\omega\epsilon' + \omega\epsilon''}} \begin{Bmatrix} 1/\cos \theta \\ \cos \theta \end{Bmatrix} = \eta \begin{Bmatrix} 1/\cos \theta \\ \cos \theta \end{Bmatrix} \quad (2.15)$$

where $\eta = \sqrt{\mu/\epsilon}$ is the intrinsic wave impedance.

This means that a bulk slab with permittivity ϵ and permeability μ can be modeled with a transmission line as in Figure 1. This is a two-port network, which can be described by its voltage-current transmission matrix (defined in Figure 2) see for instance [8, pp. 183–186] or [2, pp. 257–259]. This matrix is often termed

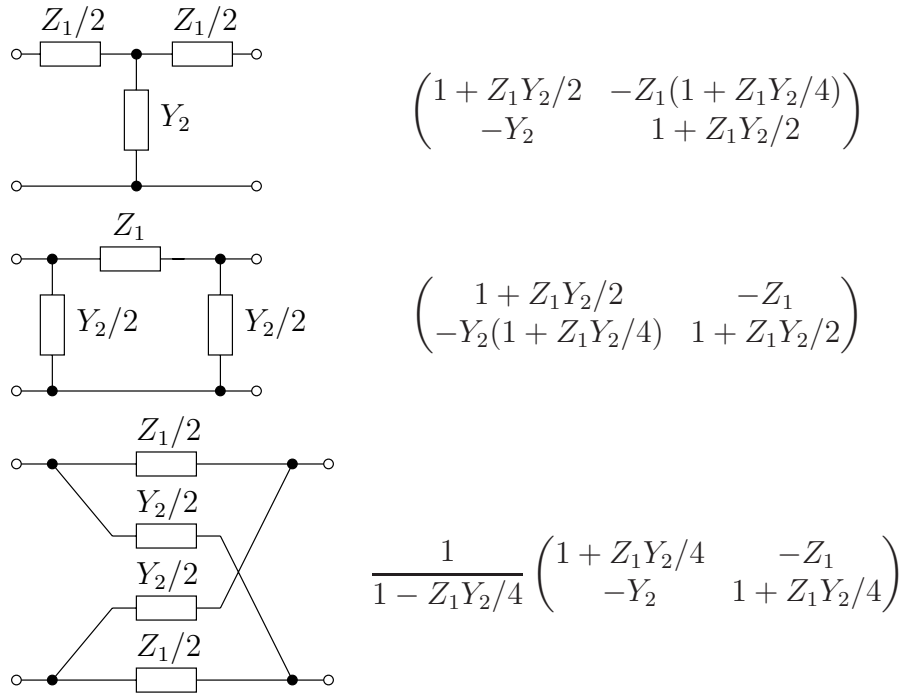


Figure 3: ABCD-matrices for symmetric T, Π , and trellis net.

the ABCD matrix, and for the transmission line it is

$$\begin{pmatrix} A & B \\ C & D \end{pmatrix} = \begin{pmatrix} \cosh(\gamma d) & -\sinh(\gamma d)Z_0 \\ -\sinh(\gamma d)Y_0 & \cosh(\gamma d) \end{pmatrix} \quad (2.16)$$

If one end of the transmission line is terminated in a load impedance Z_L , the impedance on the other end is

$$Z_{\text{in}} = Z_0 \frac{Z_L + Z_0 \tanh(\gamma d)}{Z_0 + Z_L \tanh(\gamma d)} \quad (2.17)$$

In particular, a ground plane ($Z_L = 0$) is transformed into

$$Z_{\text{in}} = Z_0 \tanh(\gamma d) = jZ_0 \tan(kd \cos \theta) \quad (2.18)$$

which typically is an inductive impedance for small d .

3 Sheets as lumped elements

In this section we study the properties of electrically thin sheets. Denoting the sheet thickness by t , this corresponds to studying $kt \rightarrow 0$. Using $\gamma = jk \cos \theta$ and keeping terms to third order in γt , we then have

$$\cosh(\gamma t) \rightarrow 1 + \frac{1}{2}(\gamma t)^2 = 1 - \frac{1}{2}k^2 t^2 \cos^2 \theta = 1 - \frac{\cos^2 \theta}{2} \omega^2 \epsilon \mu d^2 \quad (3.1)$$

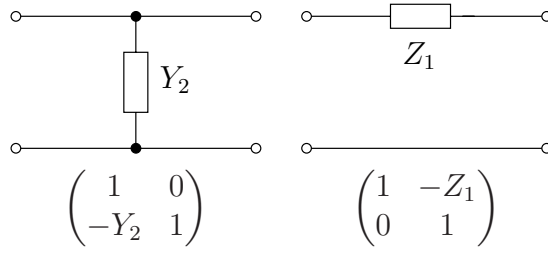


Figure 4: ABCD-matrices for a shunt and series impedance.

and

$$\begin{aligned} \sinh(\gamma t)Z_0 &\rightarrow \left(\gamma t + \frac{1}{6}(\gamma t)^3\right) Z_0 = \left(1 + \frac{(\gamma t)^2}{6}\right) jkt\eta \left\{ \begin{array}{c} 1 \\ \cos^2 \theta \end{array} \right\} \\ &= \left(1 + \frac{(\gamma t)^2}{6}\right) j\omega\mu t \left\{ \begin{array}{c} 1 \\ \cos^2 \theta \end{array} \right\} \end{aligned} \quad (3.2)$$

$$\begin{aligned} \sinh(\gamma t)Y_0 &\rightarrow \gamma t Y_0 = \left(1 + \frac{1}{6}(\gamma t)^3\right) jkt/\eta \left\{ \begin{array}{c} \cos^2 \theta \\ 1 \end{array} \right\} \\ &= \left(1 + \frac{(\gamma t)^2}{6}\right) j\omega\epsilon t \left\{ \begin{array}{c} \cos^2 \theta \\ 1 \end{array} \right\} \end{aligned} \quad (3.3)$$

Let the series impedance Z_1 and the shunt admittance Y_2 be given by the formulas (remember that these parameters will depend on frequency if the material parameters are dispersive)

$$Z_1 = j\omega\mu t \left\{ \begin{array}{c} 1 \\ \cos^2 \theta \end{array} \right\} = j\omega L t + R t \quad (3.4)$$

$$Y_2 = j\omega\epsilon t \left\{ \begin{array}{c} \cos^2 \theta \\ 1 \end{array} \right\} = j\omega C t + G t \quad (3.5)$$

where the distributed circuit parameters L , R , C , and G are defined in terms of the material parameters ϵ and μ in equations (2.12) and (2.13). It is seen that $Z_1 Y_2 = (\gamma t)^2$. The ABCD matrix for the transmission line is then, to third order in γt ,

$$\begin{pmatrix} \cosh(\gamma d) & -\sinh(\gamma d)Z_0 \\ -\sinh(\gamma d)Y_0 & \cosh(\gamma d) \end{pmatrix} \approx \begin{pmatrix} 1 + \frac{1}{2}Z_1 Y_2 & -Z_1(1 + \frac{1}{6}Z_1 Y_2) \\ -Y_2(1 + \frac{1}{6}Z_1 Y_2) & 1 + \frac{1}{2}Z_1 Y_2 \end{pmatrix} \quad (3.6)$$

We compare this matrix with the ABCD matrices for a few simple nets given in Figure 3. It is seen that the trellis net is the most accurate one, and also the most symmetric. The error occurs in the off-diagonal terms, and is $(\gamma t)^2(\frac{1}{4} - \frac{1}{6}) = (\gamma t)^2/12$. Ignoring terms of quadratic order and higher, any of the nets can be used.

The equivalent circuit for a thin sheet is particularly simple when either the series impedance Z_1 or the shunt admittance Y_2 can be neglected; we then only have the remaining shunt or series lumped element, depicted in Figure 4.

3.1 The Salisbury screen

A common case is for a material with high electric losses, $\epsilon = \epsilon' - j\epsilon''$, where $\epsilon'' \gg \epsilon'$. The equivalent circuit then consists of only a shunt conductance $Gt = \omega\epsilon''t$, which is the fundamental building block of the Salisbury screen absorber. When the losses are due to an electric conductivity, we have $Gt = \omega\epsilon''t = \sigma t$, which is independent of frequency. Since the electric conductivity σ is available in many varying orders of magnitude, resistive sheets can be found with many different values. The sheets are often characterized by the sheet resistance, $R_s = 1/(\sigma t)$, with the unit ‘‘Ohm per square’’. The name of the unit comes from the fact that the resistance of a square contacted on opposite sides is $R = \ell/(\sigma t\ell) = 1/(\sigma t) = R_s$ regardless of the physical size ℓ of the square.

The Salisbury screen consists of a resistive sheet placed at $d = \lambda/4$ in front of a ground plane, where λ is the free space wavelength at a suitable center frequency. The input impedance at distance d is

$$Z_{\text{in}} = jZ_0 \tan(kd \cos \theta) \quad (3.7)$$

which is to be shunted with a conductance Gt . The result is the new input impedance

$$Z'_{\text{in}} = \frac{1}{1/(jZ_0 \tan(kd \cos \theta)) + Gt} = \frac{1}{-jY_0 \cot(kd \cos \theta) + Gt} \quad (3.8)$$

which corresponds to the reflection coefficient

$$\Gamma = \frac{Z'_{\text{in}} - Z_0}{Z'_{\text{in}} + Z_0} = \frac{Y_0 - Y'_{\text{in}}}{Y_0 + Y'_{\text{in}}} = \frac{Y_0(1 + j \cot(kd \cos \theta)) - Gt}{Y_0(1 - j \cot(kd \cos \theta)) + Gt} \quad (3.9)$$

From this expression it can be seen that when $kd \cos \theta = \pi/2$ and $Gt = Y_0$, we have zero reflection. If Gt is independent of frequency, the bandwidth is about 25% at -20 dB reflectivity level [3, p. 316], corresponding to the bandwidth of the condition $\cot(kd \cos \theta) = 0$.

3.2 The magnetic Salisbury screen

A more rare case is a material with high magnetic losses, $\mu = \mu' - j\mu''$, where $\mu'' \gg \mu'$. A sheet of this material can then be modeled with a series resistance $Rt = \omega\mu''t$. Placing this directly on top of a ground plane, implies the input impedance of Rt and a reflection factor of

$$\Gamma = \frac{Z_{\text{in}} - Z_0}{Z_{\text{in}} + Z_0} = \frac{Rt - Z_0}{Rt + Z_0} \quad (3.10)$$

This expression is zero for all frequencies where $Rt = Z_0$. Thus, a magnetic screen can achieve infinite bandwidth if the proper frequency behavior and large enough losses can be achieved. However, magnetic losses are not available in as large contrasts as electric losses. A common case is that the real part of the permeability cannot be ignored, and we have

$$\Gamma = \frac{j\omega Lt + Rt - Z_0}{j\omega Lt + Rt + Z_0} \quad (3.11)$$

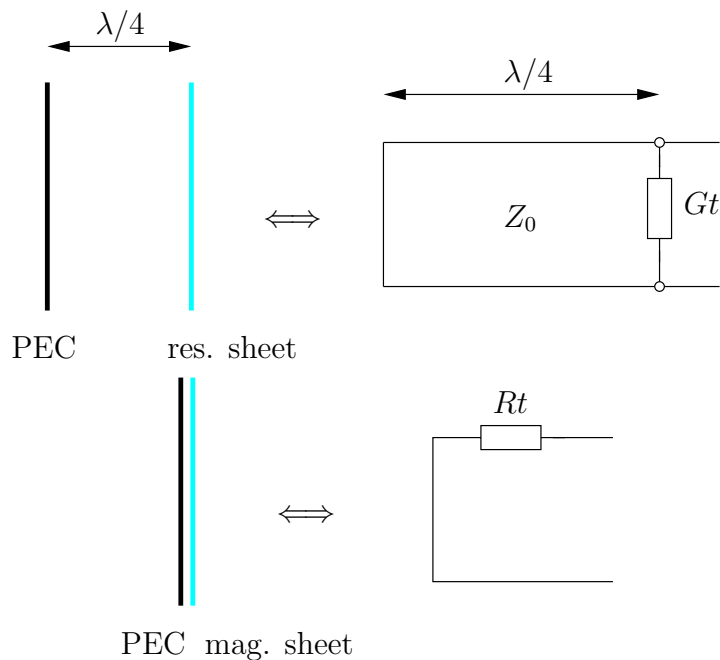


Figure 5: The Salisbury screen (top) and the magnetic Salisbury screen (bottom).

which is more realistic. Even more realistic would be to include the electric properties via a shunt admittance in the equivalent circuit for the magnetic layer.

3.3 Determining the sheet impedance from reflection data

The impedance of a single nonmagnetic sheet can be determined in a very straightforward way from reflection data, obtained either by measurements or simulations. If the sheet (with or without patterns) is situated in free space, the equivalent circuit model is given by a shunt admittance as in Figure 6.

When computing the reflection coefficient, the sheet admittance Y is shunted with the characteristic admittance Y_0 of the free space backing, which makes the reflection coefficient (at any angle of incidence) to be

$$\Gamma = \frac{Y_0 - (Y + Y_0)}{Y_0 + (Y + Y_0)} = \frac{-Y}{2Y_0 + Y} \quad (3.12)$$

From this equation, we can extract the sheet admittance in terms of the reflection coefficient:

$$Y = -Y_0 \frac{2\Gamma}{1 + \Gamma} \quad (3.13)$$

In the following section, we turn to the problem of deducing equivalent circuits which can be used to represent this admittance.

It is important to remember that the circuit parameters are not necessarily valid close to the sheet, but represent effective scattering properties of the sheet subjected to plane waves in a uniform surrounding. Typically, the sheet should be about a

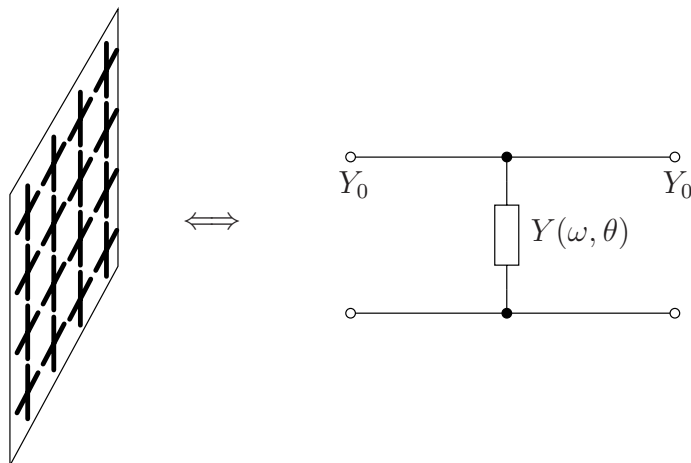


Figure 6: Equivalent circuit model for a nonmagnetic sheet. The shunt admittance is usually a function of frequency and angle of incidence, as well as polarization.

quarter wavelength from the nearest disturbance in order to be accurately modeled with fixed circuit parameters. However, even if this condition is violated, the circuit model may give an approximate behavior of the structure.

4 Patterns as reactive elements

The conventional Salisbury screen suffers from bandwidth limitations, due to the requirement of $\lambda/4$ spacing. The magnetic Salisbury screen suffers from material limitations. One way of augmenting the behavior of sheets, particularly resistive sheets, is by introducing patterns in the sheet. This pattern introduces reactive elements in the equivalent circuit for the sheet, which can be used to either a) enhance the bandwidth, or b) shrink the overall dimensions of the absorber.

4.1 Optimization approach

A numerical means of finding equivalent circuits for given pattern geometries is to compute reflection and transmission data for the pattern using full wave simulations. The data is then compared with synthetic data from a theoretical circuit model, and the parameters in the model are determined by curve fitting.

This can be done by using the program PB-FDTD (or any other suitable program) for generating the reflection data, and the matlab routine `invfreqs` to do the curve fitting. When doing this, one should not use the relation (3.13), but instead do the curve fitting to the function¹

$$\frac{1 - \Gamma}{1 + \Gamma} = \frac{Y + Y_0}{Y_0} \quad (4.1)$$

¹Thanks to Mats Gustafsson for pointing this out. This complication is due to the routine `invfreqs` being tailored to a specific class of complex functions.

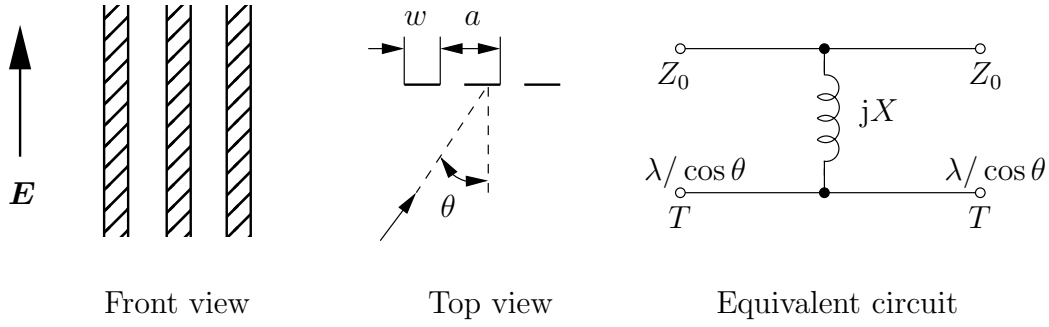


Figure 7: Geometry and equivalent circuit for inductive strips (TE polarization).

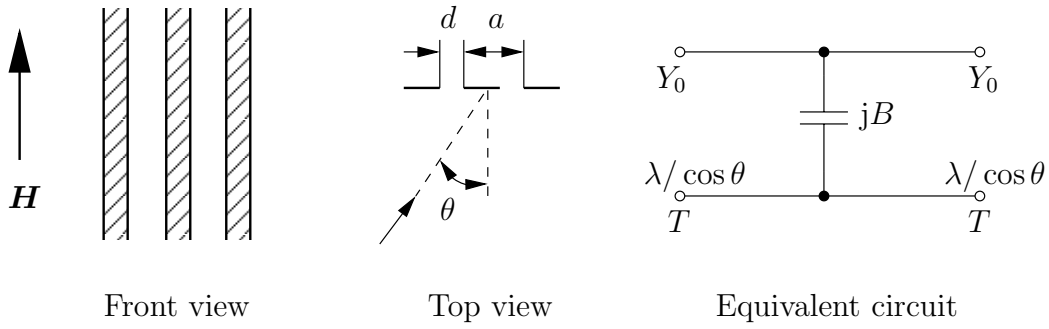


Figure 8: Geometry and equivalent circuit for capacitive strips (TM polarization).

This function is fitted to a model $p(s)/q(s)$, where p and q are polynomials in $s = j\omega$ with real-valued coefficients. The corresponding parameters for the admittance $Y(\omega, \theta)$ are then extracted from these coefficients using known expressions for Y_0 .

4.2 Strip lines

Many classical results were found during the Second World War by a massive effort in the development of radar technology, and are collected in [4, pp. 280–285]. For the case depicted in Figure 7, the strips are inductive with reactance given by [4, p. 284]

$$\frac{X}{Z_0} = \frac{a \cos \theta}{\lambda} \left\{ \ln \csc \frac{\pi w}{2a} + \frac{1}{2} \frac{(1 - \beta^2)^2 \left[\left(1 - \frac{\beta^2}{4}\right)(A_+ + A_-) + 4\beta^2 A_+ A_- \right]}{\left(1 - \frac{\beta^2}{4}\right) + \beta^2 \left(1 + \frac{\beta^2}{2} - \frac{\beta^4}{8}\right)(A_+ + A_-) + 2\beta^6 A_+ A_-} \right\} \quad (4.2)$$

$$\frac{X}{Z_0} \approx \frac{a \cos \theta}{\lambda} \left[\ln \frac{2a}{\pi w} + \frac{1}{2} (3 - 2 \cos^2 \theta) \left(\frac{a}{\lambda} \right)^2 \right], \quad \frac{w}{a} \ll 1, \quad \frac{a}{\lambda} \ll 1 \quad (4.3)$$

where

$$A_{\pm} = \frac{1}{\sqrt{1 \pm \frac{2a \sin \theta}{\lambda} - \left(\frac{a \cos \theta}{\lambda}\right)^2}} - 1 \quad (4.4)$$

$$\beta = \sin \frac{\pi w}{2a} \quad (4.5)$$

For the case depicted in Figure 8, the strips are capacitive with susceptance given by [4, p. 280]

$$\frac{B}{Y_0} = \frac{4a \cos \theta}{\lambda} \left\{ \ln \csc \frac{\pi d}{2a} + \frac{1}{2} \frac{(1 - \beta^2)^2 \left[(1 - \frac{\beta^2}{4})(A_+ + A_-) + 4\beta^2 A_+ A_- \right]}{(1 - \frac{\beta^2}{4}) + \beta^2 (1 + \frac{\beta^2}{2} - \frac{\beta^4}{8})(A_+ + A_-) + 2\beta^6 A_+ A_-} \right\} \quad (4.6)$$

$$\frac{B}{Y_0} \approx \frac{4a \cos \theta}{\lambda} \left[\ln \frac{2a}{\pi d} + \frac{1}{2} (3 - 2 \cos^2 \theta) \left(\frac{a}{\lambda} \right)^2 \right], \quad \frac{d}{a} \ll 1, \quad \frac{a}{\lambda} \ll 1 \quad (4.7)$$

where

$$A_{\pm} = \frac{1}{\sqrt{1 \pm \frac{2a \sin \theta}{\lambda} - \left(\frac{a \cos \theta}{\lambda}\right)^2}} - 1 \quad (4.8)$$

$$\beta = \sin \frac{\pi d}{2a} \quad (4.9)$$

The equivalent circuits are valid for wavelengths and angles of incidence in the range $a(1 + \sin \theta)/\lambda < 1$ [4].

These expressions form the basis for developing an analytical approach to modelling patterns in a sheet. The characteristic admittance Y_0 and impedance Z_0 in the two cases are given by

$$Z_0 = \frac{\eta_0}{\cos \theta} \quad \text{and} \quad Y_0 = \frac{1/\eta_0}{\cos \theta} \quad (4.10)$$

where $\eta_0 = \sqrt{\mu_0/\epsilon_0}$ is the free space wave impedance. Defining the capacitance C and inductance L as $B = \omega C$ and $X = \omega L$, and observing $\omega = 2\pi f = 2\pi c_0/\lambda = 2\pi/(\lambda\sqrt{\epsilon_0\mu_0})$, we find

$$L = \frac{X}{\omega} = \frac{Z_0 X}{\omega Z_0} = \frac{\lambda \eta_0}{2\pi c_0 \cos \theta} \frac{X}{Z_0} = \frac{\lambda \mu_0}{2\pi \cos \theta} \frac{X}{Z_0} = \frac{a \mu_0}{2\pi} \left\{ \ln \csc \frac{\pi w}{2a} + \dots \right\} \quad (4.11)$$

$$C = \frac{B}{\omega} = \frac{Y_0 B}{\omega Y_0} = \frac{\lambda/\eta_0}{2\pi c_0 \cos \theta} \frac{B}{Y_0} = \frac{\lambda \epsilon_0}{2\pi \cos \theta} \frac{B}{Y_0} = \frac{4a \epsilon_0}{2\pi} \left\{ \ln \csc \frac{\pi d}{2a} + \dots \right\} \quad (4.12)$$

It is seen that both the circuit parameters depend on the geometry parameters through the function

$$f \left(\frac{d}{a}, \frac{a}{\lambda}, \theta \right) = \left\{ \ln \csc \frac{\pi d}{2a} + \dots \right\} \quad (4.13)$$

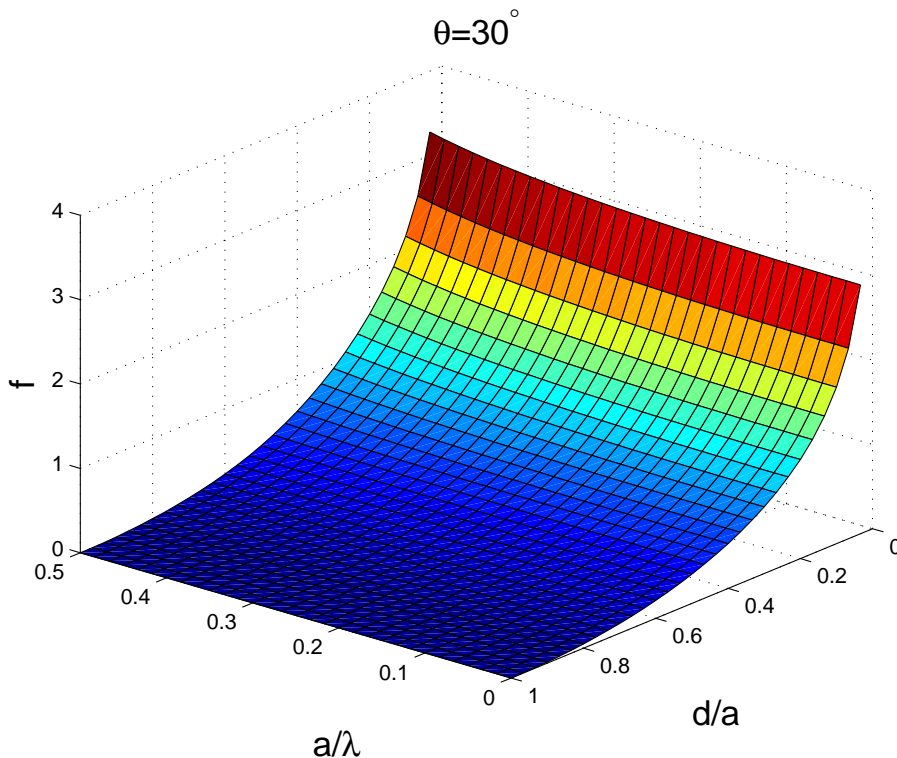


Figure 9: The function $f(\frac{d}{a}, \frac{a}{\lambda}, \theta)$ for $\theta = 30^\circ$. The function does not change appreciably with θ .

as

$$L = \frac{a\mu_0}{2\pi} f\left(\frac{w}{a}, \frac{a}{\lambda}, \theta\right) \quad (4.14)$$

$$C = \frac{4a\epsilon_0}{2\pi} f\left(\frac{d}{a}, \frac{a}{\lambda}, \theta\right) \quad (4.15)$$

It is interesting to characterize f as a function of its three arguments. In Figure 9, we have plotted it as a function of a/λ and d/a for $\theta = 30^\circ$. The function is relatively insensitive to changes in θ , and depends most strongly on the parameter d/a .

This can be given an immediate interpretation in terms of how the circuit parameters change with the dimensions of the strips:

- To make the inductance L large, the ratio w/a should be small, *i.e.*, the width of the strips should be small.
- To make the capacitance C large, the ratio d/a should be small, *i.e.*, the gap between the strips should be small.

Both L and C are directly proportional to the period a , which must be smaller than half a wavelength.

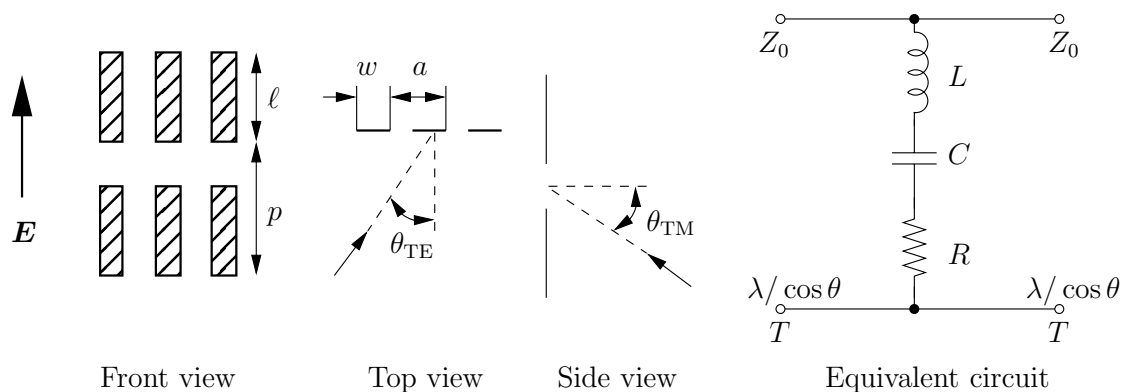


Figure 10: Finite dipole. Observe that the incidence plane changes depending on whether we study TE or TM polarization, since the dipoles would be practically invisible for other cases.

4.3 Dipoles

The simplest possible pattern is the finite length dipole as depicted in Figure 10. The equivalent circuit must be a series circuit, since the pattern is a band stop filter.

The dipole pattern is characterized by five design parameters: the periodicity lengths a and p , the dipole width w and length ℓ , and the sheet resistance $R_s = 1/(\sigma t)$. To simplify matters, we choose $a = p$ and choose $\ell \approx a \gg w$, *i.e.*, we study elongated dipoles in a quadratic unit cell. The dipoles are then practically invisible except when the electric field has a component parallel to the dipole.

4.4 Crossed dipoles

To make the dipole pattern independent of polarization, it is common to choose a pattern consisting of crossed dipoles. Essentially, this configuration can be analyzed as a superposition of linear dipoles.

4.5 Patches

Another simple pattern is to use patches, which might be regarded as fat dipoles, see Figure 11. Once again, the equivalent circuit should be a series circuit, since the pattern is a band stop circuit.

5 Design of absorbers

5.1 Physical limitations

Konstantin Rozanov has written a very interesting paper on the ultimate thickness to bandwidth ratio of radar absorbers [9]. Based simply on the assumption of linear

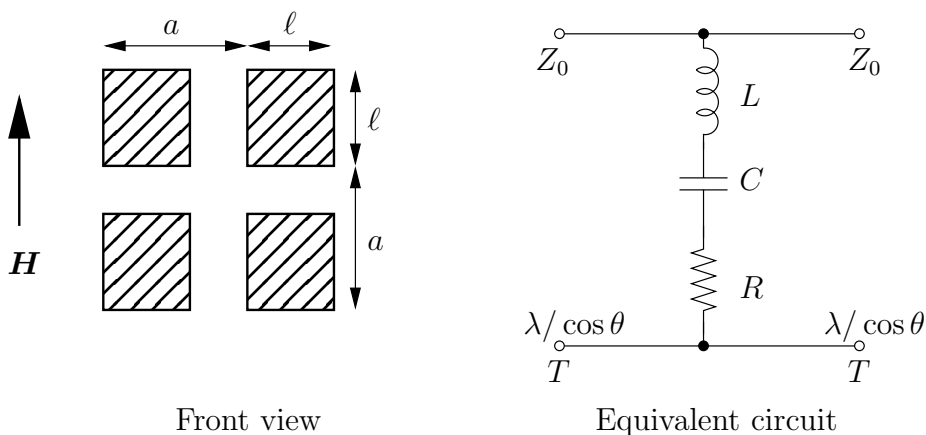


Figure 11: A pattern of square patches.

materials and the principle of causality, he derives the result

$$\int_0^\infty \ln \left(\frac{1}{|\Gamma(\lambda)|} \right) d\lambda \leq 2\pi^2 \sum_i \mu_{s,i} d_i \quad (5.1)$$

where $\mu_{s,i}$ is the static relative permeability of layer i , and d_i is the thickness of the corresponding layer. For nonmagnetic media, the right hand side is simply $2\pi^2 d$, where d is the total thickness of the absorber.

This relation states that the reflection coefficient can be small only in a limited band. This can be estimated by choosing a reflection profile which is constant Γ_0 in the band $\lambda_1 < \lambda < \lambda_2$, indicating (for nonmagnetic absorbers)

$$\ln \left(\frac{1}{|\Gamma_0|} \right) (\lambda_2 - \lambda_1) \leq 2\pi^2 d \quad (5.2)$$

This can be expressed as a bandwidth in frequency through $\lambda_2 - \lambda_1 = c_0/f_2 - c_0/f_1 = \frac{c_0}{f_1 f_2} (f_1 - f_2)$.

5.2 Single layer

In this section, we say a few short words on the design of a classical circuit analog absorber. The situation is typically that at a certain height h above a ground plane, we should place a circuit analog sheet. The situation can be modeled as in Figure 12, where the admittance of the ground plane in combination with the transmission line of length h is

$$Y_h(\omega) = -jY_0 \cot(kh \cos \theta) \quad (5.3)$$

At the frequency where the distance to the ground plane is a quarter wavelength, *i.e.*, $\omega_h = k_h c_0$ where $k_h h \cos \theta = \pi/2$, we can make a Taylor series expansion of this to find

$$Y_h(\omega) = -jY_0 (0 - (k - k_h)h \cos \theta + O((k - k_h)^2)) \approx jY_0(\omega - \omega_h)c_0^{-1}h \cos \theta \quad (5.4)$$

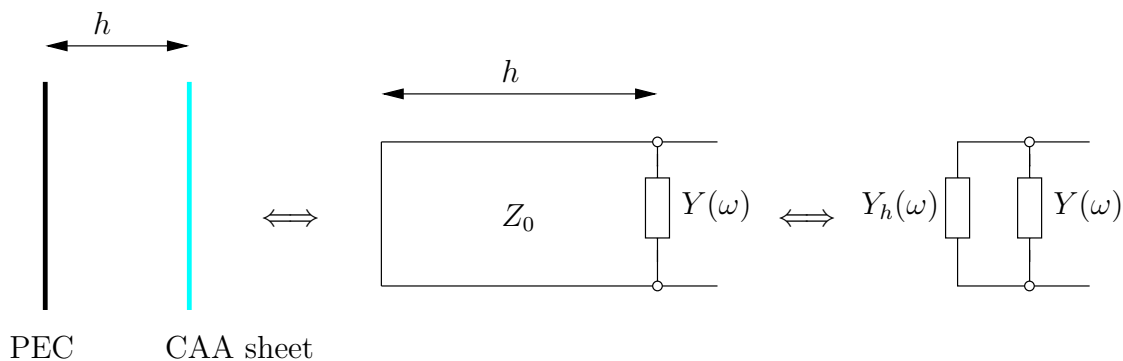


Figure 12: Typical situation for a CAA sheet.

To obtain good absorption over a broad interval, the CAA admittance $Y(\omega)$ should be chosen so that $Y(\omega) + Y_h(\omega) \approx Y_0$ in as broad an interval as possible.

The CAA sheet is modeled with a series circuit, which has the admittance

$$\begin{aligned}
 Y(\omega) &= \frac{1}{R + j\omega L + \frac{1}{j\omega C}} = \frac{1/R}{1 + jQ \left(\frac{\omega}{\omega_0} - \frac{\omega_0}{\omega} \right)} = \frac{1/R}{1 + jQ \frac{\omega + \omega_0}{\omega_0 \omega} (\omega - \omega_0)} \\
 &= \frac{1}{R} - j \frac{Q}{R} \frac{2}{\omega_0} (\omega - \omega_0) + O((\omega - \omega_0)^2) \quad (5.5)
 \end{aligned}$$

where the quality factor is $Q = \sqrt{L/C}/R$ and the resonance frequency is $\omega_0 = 1/\sqrt{LC}$. To obtain broad band matching, we should not make an exact match at any frequency, but instead try to achieve a slight mismatch in a broad band. We now outline a simple strategy for this.

We choose the resonance frequency ω_0 equal to ω_h , which makes the reflection factor at this frequency real:

$$\Gamma(\omega_0) = \frac{Y_0 - (Y_h(\omega_0) + Y(\omega_0))}{Y_0 + Y_h(\omega_0) + Y(\omega_0)} = \frac{Y_0 - 1/R}{Y_0 + 1/R} \quad (5.6)$$

Let this reflection factor be negative, $\Gamma(\omega_0) = -\Gamma_0$ where Γ_0 is a positive real number giving the typical reflection level. This implies the resistance should be chosen as

$$R = \frac{1}{Y_0} \frac{1 - \Gamma_0}{1 + \Gamma_0} \quad (5.7)$$

Next, we set the imaginary part of $Y_h(\omega) + Y(\omega)$ to zero at first order in $\omega - \omega_0$, implying

$$Y_0 c_0^{-1} h \cos \theta = \frac{2Q}{R \omega_0} = \frac{2\sqrt{L/C}/R}{R/\sqrt{LC}} = \frac{2L}{R^2} \quad (5.8)$$

which means the inductance should be chosen as

$$L = \frac{R^2 Y_0 c_0^{-1} h \cos \theta}{2} = \frac{c_0^{-1} h \cos \theta}{2 Y_0} \left(\frac{1 - \Gamma_0}{1 + \Gamma_0} \right)^2 \quad (5.9)$$

Finally, the condition $\omega_0 = \omega_h$, or $1/\sqrt{LC} = \frac{\pi}{2}(c_0^{-1}h \cos \theta)^{-1}$, means

$$C = \frac{1}{L} \left(\frac{c_0^{-1}h \cos \theta}{\pi/2} \right)^2 = 2Y_0 \frac{c_0^{-1}h \cos \theta}{\pi^2/4} \left(\frac{1 + \Gamma_0}{1 - \Gamma_0} \right)^2 \quad (5.10)$$

Summarizing our results, we have

$$R = \frac{1}{Y_0} \frac{1 - \Gamma_0}{1 + \Gamma_0} = \frac{1 - \Gamma_0}{1 + \Gamma_0} \eta \left\{ \begin{array}{c} 1/\cos \theta \\ \cos \theta \end{array} \right\} \quad (5.11)$$

$$C = 2Y_0 \frac{c_0^{-1}h \cos \theta}{\pi^2/4} \left(\frac{1 + \Gamma_0}{1 - \Gamma_0} \right)^2 = \left(\frac{1 + \Gamma_0}{1 - \Gamma_0} \right)^2 \frac{8}{\pi^2} \epsilon h \left\{ \begin{array}{c} \cos^2 \theta \\ 1 \end{array} \right\} \quad (5.12)$$

$$L = \frac{c_0^{-1}h \cos \theta}{2Y_0} \left(\frac{1 - \Gamma_0}{1 + \Gamma_0} \right)^2 = \left(\frac{1 - \Gamma_0}{1 + \Gamma_0} \right)^2 \frac{1}{2} \mu h \left\{ \begin{array}{c} 1 \\ \cos^2 \theta \end{array} \right\} \quad (5.13)$$

where again the top alternative is for TE polarization and the lower for TM. These formulas may serve as a reasonable starting point to design the CAA sheet, for instance by using the optimization approach in Section 4.1.

In Figure 13 we compare the reflection for a Salisbury screen with a circuit analog sheet where the circuit parameters have been chosen for normal incidence and -20 dB reflection level according to the formulas just derived. It is seen that the circuit model is very accurate for low frequencies, as could be expected, but the deviation is greater for frequencies above the resonance frequency. In order to improve the design, one could try to lower the resonance frequency of the pattern by increasing the capacitance, *e.g.*, by decreasing the gap between the outer bars. The result of this procedure is depicted in Figure 14, where it is seen that now the -20 dB bandwidth of the absorber is now closer to the physical limit.

It should be mentioned that the choice of circuit parameters made here, may not correspond to a design with reasonable tolerances. The changes in geometry between Figure 13 and Figure 14 are only a few pixels in the FDTD-grid, and still give a noticeable change. The study of the sensitivity of the design is a further (nontrivial) chapter in the development of circuit analog absorbers, and is not considered here.

5.3 Multiple layers

For even broader absorption band, a multilayer approach can be useful. The circuit analog approach can be useful to find a suitable basic design based on simple circuit models for each sheet, connected by transmission lines. At this stage good knowledge of broad band matching techniques from microwave circuit theory is beneficial. For instance, plotting the reflection coefficient in the Smith chart provides an intuitive means of analyzing the problem. This simple (and very fast) circuit model can then be used to find a good starting point for a full wave optimizer for the final design.

6 Discussion and conclusions

We have demonstrated how circuit models can be used to describe wave propagation in stratified structures, and how this can be utilized to give simple design guidelines

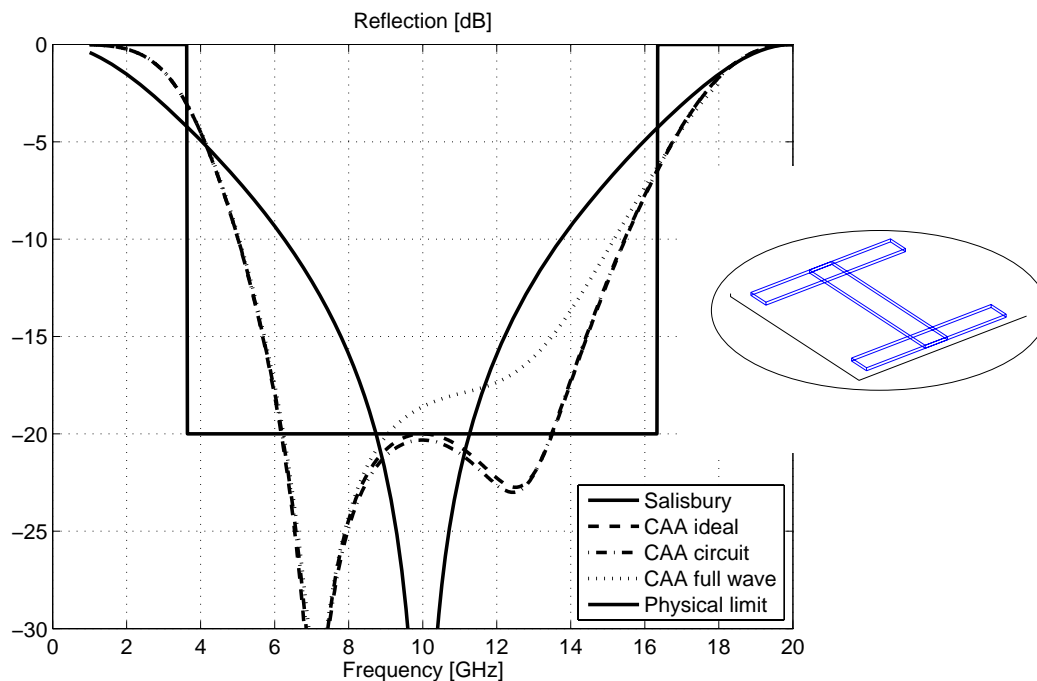


Figure 13: Comparison between a Salisbury screen and a circuit analog absorber (total height is 7.5 mm, normal incidence). The ideal circuit parameters are $R = 308 \Omega$, $C = 80.4 \text{ fF}$, and $L = 3.15 \text{ nH}$. These parameters are approximately achieved by the geometry depicted on the right, where the procedure described in Section 4.1 predicts $R = 311 \Omega$, $C = 80.4 \text{ fF}$, and $L = 3.16 \text{ nH}$. These parameters are used in a circuit model, and the full wave results (simulated with PB-FDTD) are also displayed. The physical limit (5.2) is represented by the square box, demonstrating that there is room for improvement on this design.

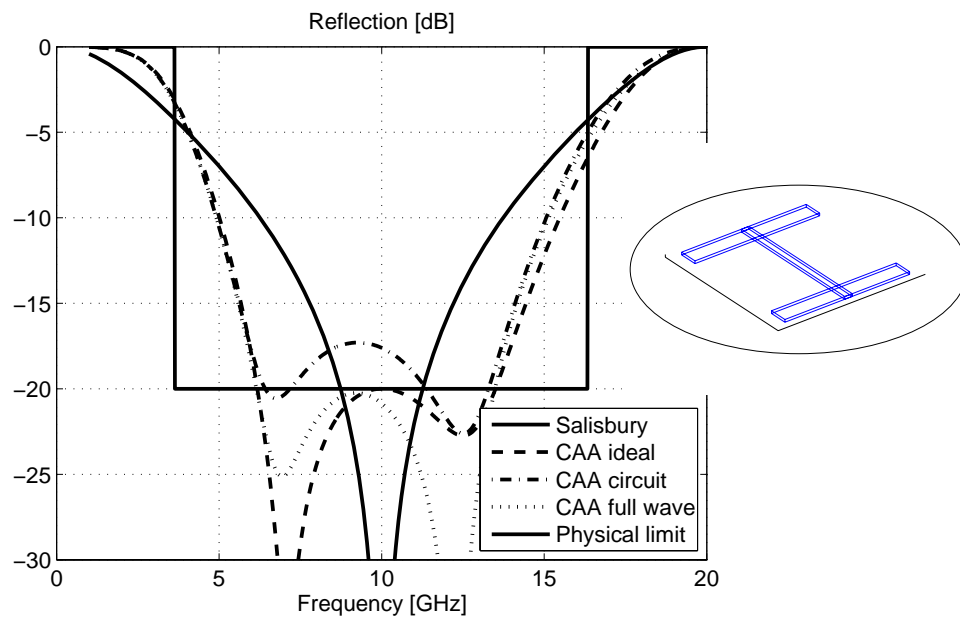


Figure 14: A version of the previous CAA pattern with more slender center part, and lower resistance per square. This provides higher inductance and therefore lower resonance frequency than the structure in Figure 13. The circuit parameters, calculated by the optimization approach in Section 4.1, are $R = 319 \Omega$, $C = 79.1 \text{ fF}$, and $L = 4.35 \text{ nH}$.

for absorbing structures. The circuit models have a long history, typically being derived or estimated analytically in a time when no computers were available. In present time, the design of patterns in a resistive sheet to obtain desired circuit parameters is much more feasible, although the analytical approaches still serve to give good estimates of what is possible to achieve.

We have not discussed the problem of oblique incidence explicitly, though it can be seen that the circuit parameters typically may scale as $\cos^2 \theta$ for one polarization, but not for the other. Another complication is that the effective wavelength and characteristic impedance of the equivalent transmission lines scale with $\cos \theta$ or $1/\cos \theta$. How to deal with these problems are treated in [7].

As can be seen in Figure 13, the performance of the classical Salisbury screen is far from optimal. Even though the situation is significantly improved by adding patterns in the resistive sheet, there is still room for more improvement.

References

- [1] R. E. Collin. *Field Theory of Guided Waves*. IEEE Press, New York, second edition, 1991.
- [2] R. E. Collin. *Foundations for Microwave Engineering*. McGraw-Hill, New York, second edition, 1992.
- [3] E. F. Knott, J. F. Shaeffer, and M. T. Tuley. *Radar Cross Section*. SciTech Publishing Inc., 5601 N. Hawthorne Way, Raleigh, NC 27613, 2004.
- [4] N. Marcuvitz. *Waveguide Handbook*. McGraw-Hill, New York, 1951.
- [5] B. Munk. *Frequency Selective Surfaces: Theory and Design*. John Wiley & Sons, New York, 2000.
- [6] B. Munk. *Finite Antenna Arrays and FSS*. John Wiley & Sons, New York, 2003.
- [7] B. A. Munk, P. Munk, and J. Pryor. On designing Jaumann and circuit analog absorbers (CA absorbers) for oblique angle of incidence. *IEEE Trans. Antennas Propagat.*, **55**(1), 186–193, January 2007.
- [8] D. M. Pozar. *Microwave Engineering*. John Wiley & Sons, New York, third edition, 2005.
- [9] K. N. Rozanov. Ultimate thickness to bandwidth ratio of radar absorbers. *IEEE Trans. Antennas Propagat.*, **48**(8), 1230–1234, August 2000.